Infrared conductivity of a one-dimensional charge-ordered state: Quantum lattice effects

C. A. Perroni, V. Cataudella, G. De Filippis, G. Iadonisi, V. Marigliano Ramaglia, and F. Ventriglia
Coherentia-INFM and Dipartimento di Scienze Fisiche, Università degli Studi di Napoli "Federico II," Complesso Universitario Monte Sant'Angelo, Via Cintia, I-80126 Napoli, Italy

(Received 26 August 2002; revised manuscript received 6 February 2003; published 9 June 2003)

The optical properties of the charge-ordering (CO) phase of the one-dimensional (1D) half-filled spinless Holstein model are derived at zero temperature within a well-known variational approach improved including second-order lattice fluctuations. Within the CO phase, the static lattice distortions give rise to the optical interband gap, that broadens as the strength of the electron-phonon (el-ph) interaction increases. The lattice fluctuation effects induce a long subgap tail in the infrared conductivity and a wide band above the gap energy. The first term is due to the multiphonon emission by the charge carriers and the second to the interband transitions accompanied by the multiphonon scattering. The results show a good agreement with experimental spectra of quasi-1D conductors such as $K_{0.3}MoO_3$ and $(TaSe_4)_2I$.

DOI: 10.1103/PhysRevB.67.214301 PACS number(s): 71.38.−k, 71.35.Cc, 71.30.+h

In recent years there has been a renewed interest in charge density wave (CDW) materials.[1] The transition to a charge-ordering (CO) phase is common to a wide range of compounds,[2] including many quasi-1D materials such as organic conjugated polymers, charge transfer salts, molybdenum bronzes, and MX chains.[1–5] These materials undergo a Peierls instability driven by the el-ph interaction in the half-filled band case. For most quasi-1D systems, the lattice zero-point motion is comparable to the Peierls lattice distortion, so quantum lattice fluctuations must be taken into account to satisfactorily describe spectral, transport and optical properties.[6–8] In particular the study of the optical absorption of CO materials represents a very useful tool to extract the gap energy and, in general, to investigate the properties of the ordered state.[1,9–11] In this framework, the experimental measurements have pointed out that the lattice fluctuation effects can remove the inverse square-root singularity expected for the case of a static distorted lattice[12] profoundly affecting the conductivity spectra.[6,13,14] Actually these effects give rise to the subgap optical absorption seen in these materials where a significant tail below the maximum of the interband transition term is measured. Moreover the optical absorption above the interband optical gap band also presents deviations from the behavior obtained within the mean-field approach of the static lattice.[13]

The challenge of understanding the effect of quantum lattice fluctuations on the Peierls dimerization and the absorption spectra has determined an intense study of the Holstein model[15] that is a typical el-ph coupling model developing a CO state at half filling. Actually the Holstein Hamiltonian has been investigated by using various techniques, such as Monte Carlo simulations,[16,17] renormalization-group analysis,[18,19] variational method,[20–22] density-matrix renormalization group[23] and exact diagonalization.[24] These studies reveal that, in the spinless case, there is a quantum phase transition from a Luttinger liquid (metallic) phase to an insulating phase with CDW long-range order. Because of limited system sizes in numerical approaches, except for the antiadiabatic regime, the behavior of the conductivity spectra is not well determined, so the extraction of the gap from the optical data is not precise.[24] However, through exact diagonalization methods, the spectral weight of the conductivity can be deduced showing the onset of the infrared absorption for lattices of a few sites. Recently, an analytical variational approach,[21,22] valid in the weak el-ph coupling regime, has been developed to study the phase diagram and the optical conductivity of the Holstein model. The employed approximation has different effects on the phase diagram and the optical properties. In fact, the maximum in the optical spectra does not directly correspond to the gap calculated within the variational approach. Actually the peak position of the optical conductivity is higher than the gap with an energy separation of the order of the electron transfer integral in the adiabatic limit. Therefore, experimental findings of a tail in the optical spectra below the gap energy (corresponding to the maximum of experimental conductivities) does not find a clear explanation within previous approaches.

In this paper we employ the variational scheme proposed for the one-dimensional (1D) half-filled spinless Holstein model by Zheng, Feinberg, and Avignon[20] (ZFA) in order to calculate the spectral properties and the infrared response. We note that the ZFA method improves the mean-field solution showing a good agreement with other numerical works.[16,17,23,24] Actually this approach is able to introduce lattice fluctuations on the mean-field Peierls solution since the lattice deformation is allowed to follow the electrons instantaneously. The calculated conductivity spectra are characterized by a transfer of spectral weight from low to high energies and by a broadening of the optical interband gap, with increasing the el-ph coupling. The effect of the quantum lattice fluctuations is able to determine in the infrared conductivity a subgap absorption term near the phonon energy and a wide band above the gap energy. The first contribution is due to the multiphonon emission by the charge carriers, the second to the interband transitions accompanied by the multiphonon scattering. The inclusion of lattice fluctuation effects beyond the ZFA approach is able to smooth the inverse square-root singularity of the ZFA and mean-field conductivity. Moreover these effects strengthen the features of the conductivity below and above the gap already found in the ZFA approach inducing an actual subgap tail. Therefore lattice fluctuations influence the optical absorption at the

 ©2003 The American Physical Society

low-energy subgap, at the gap and at the high-energy scale above the interband optical gap term. These features are found in the measured spectra of quasi-1D conductors such as $K_{0.3}MoO_3$ and $(TaSe_4)_2I$.[13,14]

In Sec. I the model and the ZFA variational approach are briefly reviewed. In Sec. II the spectral properties are deduced in order to characterize the quasiparticle gap of the CO phase. In Sec. III the infrared spectra obtained within the ZFA approach are discussed. Finally, in Sec. IV the effects of lattice fluctuations beyond the ZFA approach are analyzed.

I. MODEL AND ZFA VARIATIONAL APPROACH

In this paper we deal with the 1D spinless Holstein model[15] at half filling. The Holstein Hamiltonian is

$$H=-t\sum_{\langle i,j\rangle} c_i^\dagger c_j+\omega_0\sum_i a_i^\dagger a_i+g\omega_0\sum_i c_i^\dagger c_i(a_i+a_i^\dagger) - \mu\sum_i c_i^\dagger c_i . \tag{1}$$

Here t is the electron transfer integral between nearest neighbor (NN) sites $\langle i,j\rangle$, $c_i^\dagger(c_i)$ creates (destroys) an electron at the ith site, and μ is the chemical potential. In the second term of Eq. (1) $a_i^\dagger(a_i)$ is the creation (annihilation) phonon operator at the site i, ω_0 denotes the frequency of the optical phonon mode, and the parameter g represents the coupling constant between electrons and phonons. The dimensionless parameter λ

$$\lambda=\frac{g^2\omega_0}{2t}, \tag{2}$$

indicating the ratio between the small polaron binding energy and the energy gain of an itinerant electron on a rigid lattice, is useful to measure the strength of the el-ph interaction in the adiabatic regime. We consider spinless electrons since they, even if at a very rough level, mimic the action of an on-site Coulomb repulsion preventing the formation of local pairs. Actually, for one dimensional systems in the limit of infinite local repulsion U, the charge sector of the Hubbard model maps onto a spinless model, therefore the spinless Holstein model can be considered as a reliable model for typical one-dimensional systems.

The hopping of electrons is supposed to take place between the equivalent nn sites of a 1D lattice separated by the distance a. The units are such that the Planck constant $\hbar=1$ and the lattice parameter $a=1$.

As stressed in the original ZFA paper,[20] the starting point of the approach is the consideration that the strong coupling and infinite phonon frequency limit of the model are described by polarons. The ZFA approach extends the polaron formation to intermediate regimes recovering the mean-field solution of the zero phonon frequency limit. Following the ZFA variational scheme, three successive canonical transformations are performed in order to treat the electron-phonon interaction variationally and to introduce the charge-ordering solution.

The first transformation is the variational Lang-Firsov unitary one[25]

$$U_1=\exp\left[g\sum_j (fc_j^\dagger c_j+\Delta_j)(a_j-a_j^\dagger)\right], \tag{3}$$

where f and Δ_j are variational parameters. The quantity f controls the degree of the antiadiabatic polaronic effect since the lattice deformation is allowed to follow instantaneously the electrons. Moreover Δ_j denotes a displacement field describing lattice distortions due to the average electron motion. At half filling the charge-ordered solution is obtained by assuming

$$\Delta_i=\Delta+\Delta_{CO}e^{iQR_i}, \tag{4}$$

where Δ represents the lattice distortion unaffected by the instantaneous position of electrons and Δ_{CO} the additional local lattice distortion due to the Peierls dimerization with $Q=\pi$. The second transformation is

$$U_2=\exp\left[\alpha\sum_j (a_j^\dagger a_j^\dagger-a_j a_j)\right], \tag{5}$$

where the variational parameter α determines a phonon frequency renormalization.

The transformed Hamiltonian $\tilde{H}=U_2^{-1}U_1^{-1}HU_1U_2$ is

$$\tilde{H}=-t\sum_{\langle i,j\rangle} X_i^\dagger X_j c_i^\dagger c_j+\bar{\omega_0}\sum_i a_i^\dagger a_i+L\omega_0\sinh^2(2\alpha) +g^2\omega_0\sum_i \Delta_i^2+\omega_0\sinh(2\alpha)\cosh(2\alpha)\sum_i (a_i^\dagger a_i^\dagger+a_i a_i) -g\omega_0 e^{2\alpha}\sum_i \Delta_i(a_i+a_i^\dagger) +g\omega_0(1-f)e^{2\alpha}\sum_i c_i^\dagger c_i(a_i+a_i^\dagger)+\sum_i c_i^\dagger c_i(\eta_i-\mu), \tag{6}$$

where we have introduced the phonon operator X_i

$$X_i=\exp[gfe^{-2\alpha}(a_i-a_i^\dagger)], \tag{7}$$

the renormalized phonon frequency $\bar{\omega_0}=\omega_0\cosh(4\alpha)$, the number of lattice sites L, and the quantity η_i

$$\eta_i=g^2\omega_0 f(f-2)+2g^2\omega_0(f-1)\Delta_i . \tag{8}$$

In the ZFA approach the energy is deduced introducing a test Hamiltonian characterized by noninteracting electron and phonon degrees of freedom such that $\langle\tilde{H}-H_{test}\rangle_t=0$, where $\langle\ \rangle_t$ indicates the mean value obtained by using the ground state of H_{test}. The test Hamiltonian is given by

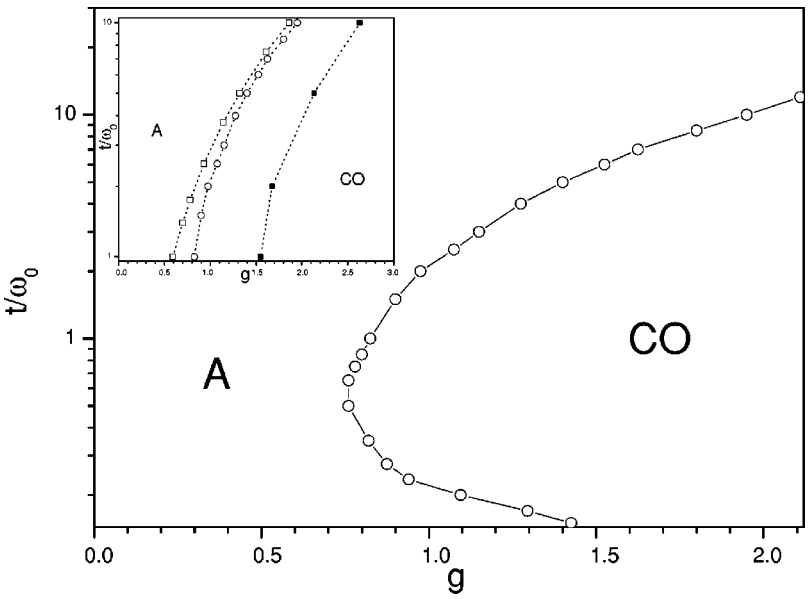

FIG. 1. The phase diagram of the system. The line separates the CO from the *A* phase, that represents the disordered normal state. In the inset, the transition line between the CO and the disordered *A* phase calculated in the mean-field (white squares), ZFA (white circles), and DMRG approach (black squares).

$$H_{\text{test}} = -t_{\text{eff}} \sum_{\langle i,j \rangle} c_i^\dagger c_j + \bar{\omega}_0 \sum_i a_i^\dagger a_i + L\omega_0 \sinh^2(2\alpha) + Lg^2\omega_0(\Delta^2 + \Delta_{\text{CO}}^2) - 2g^2\omega_0\Delta_{\text{CO}}(1-f) \times \sum_i e^{iQR_i} c_i^\dagger c_i - \mu_0 \sum_i c_i^\dagger c_i , \tag{9}$$

where the subsidiary chemical potential μ_0 is

$$\mu_0 = \mu - g^2\omega_0 f(f-2) + 2g^2\omega_0(f-1)\Delta. \tag{10}$$

The quantity $t_{\text{eff}} = te^{-S}$ denotes the effective transfer integral, where the quantity

$$S = g^2 f^2 e^{-4\alpha} \tag{11}$$

controls the band renormalization due to the polaron formation. The electronic part of the test Hamiltonian is diagonalized by a third canonical Bogoliubov transformation[20] yielding

$$\tilde{H}_{\text{test}} = \sum_{k \epsilon \text{NZ}} (\xi_k^{(+)} - \mu_0) d_k^\dagger d_k + \sum_{k \epsilon \text{NZ}} (\xi_k^{(-)} - \mu_0) p_k^\dagger p_k + \bar{\omega}_0 \sum_q a_q^\dagger a_q + L\omega_0 \sinh^2(2\alpha) + Lg^2\omega_0(\Delta^2 + \Delta_{\text{CO}}^2), \tag{12}$$

where $d_k^\dagger(d_k)$ creates (destroys) a quasiparticle in the upper band $\xi_k^{(+)} = \sqrt{\tilde{\epsilon}_k^2 + E^2}$, $p_k^\dagger(p_k)$ creates (destroys) a quasiparticle in the lower band $\xi_k^{(-)} = -\sqrt{\tilde{\epsilon}_k^2 + E^2}$, and $\tilde{\epsilon}_k$ is the polaronic band. We note that NZ indicates the new (Brillouin) zone defined by the condition $\tilde{\epsilon}_k \leqslant 0$. In the CO phase a gap opens between the upper and lower bands in the quasiparticle spectrum and it is twice the quantity

$$E = 2g^2\omega_0\Delta_{\text{CO}}(1-f). \tag{13}$$

Within the variational approach the kinetic energy mean value $\bar{E}_{\text{kin}}$ is

$$\bar{E}_{\text{kin}} = \langle \hat{T} \rangle = -\int_{-\tilde{W}}^{0} d\epsilon g(\epsilon) \frac{\epsilon^2}{\sqrt{\epsilon^2 + E^2}}, \tag{14}$$

where $\tilde{W} = 2t_{\text{eff}}$ is the renormalized band half width, $g(\epsilon)$ the 1D density of states, and the electron order parameter m_e is given by

$$m_e = \left(\frac{1}{L}\right) \sum_i e^{i\vec{Q}\cdot\vec{R}_i} \langle c_i^\dagger c_i \rangle = E \int_{-\tilde{W}}^{0} d\epsilon \frac{g(\epsilon)}{\sqrt{\epsilon^2 + E^2}}. \tag{15}$$

The CO phase is characterized by an order parameter other than zero.

In Fig. 1 we report the phase diagram[20] derived within the ZFA approach in the thermodynamic limit. The ordered state is separated with a transition line by the *A* phase that represents the disordered phase ($\Delta_{\text{CO}} = 0$). Previous studies[17,21,23,24] have pointed out that the normal state has the properties of a Luttinger liquid. This has been verified also by using the ZFA wave function and making a finite-size scaling analysis.[24] In the inset of Fig. 1, there is a comparison between the transition lines calculated in a mean-field approach (white squares), ZFA approach (white circles), and DMRG approach[23] (black squares). Here "mean-field approach" means that we are neglecting the effect of polaron formation ($f = 0$, $\alpha = 0$). In the ranges of parameters relevant for quasi-one-dimensional materials, the ZFA approach improves the mean-field solution since the CO phase is stable for larger values of the el-ph couplings. However the lattice fluctuation effects introduced by this approach are not sufficient to obtain transition lines comparable with those of DMRG approach. This indicates that quantum fluctuation effects beyond the ZFA scheme are not negligible and can play a role also in the calculation of the dynamical properties of the model.

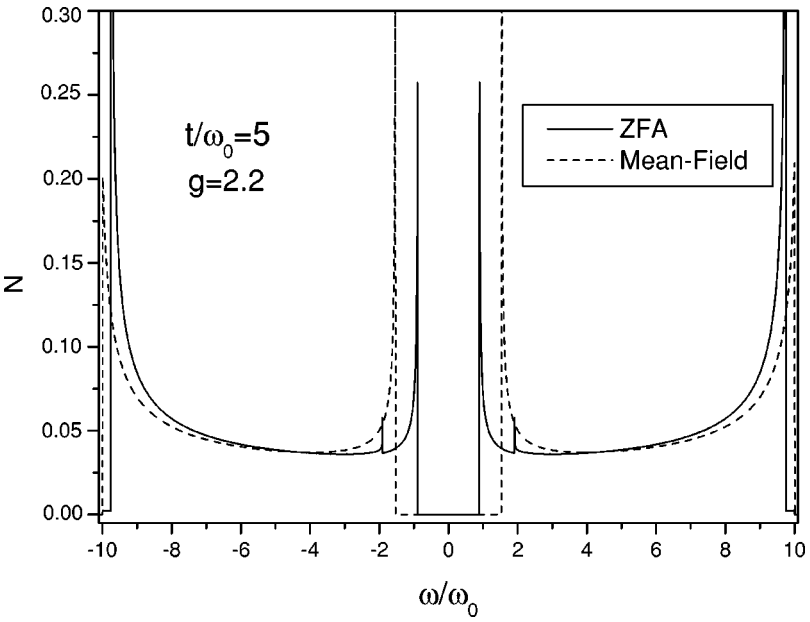

FIG. 2. The renormalized density of states derived in the ZFA (solid line) and mean-field approach (dashed line) at $t=5\omega_0$ and $g=2.2$ as a function of the energy (in units of ω_0).

II. SPECTRAL PROPERTIES WITHIN ZFA APPROACH

In this section we calculate the spectral properties within the ZFA approach. They are discussed in order to characterize the gap in the quasiparticle spectrum.

The electron retarded Green's function can be disentangled into electronic and phononic terms[26] by using the test Hamiltonian (9), hence

$$G_{\rm ret}(k,t)=e^{-S}G_{\rm ret}^{(co)}(k,t)+e^{-S}[\exp(Se^{-i\bar{\omega}_0 t})-1]\times\frac{1}{L}\sum_{k_1\epsilon {\rm NZ}}G_{\rm ret}^{(+)}(k_1,t)+e^{-S}[\exp(Se^{i\bar{\omega}_0 t})-1]\times\frac{1}{L}\sum_{k_1\epsilon {\rm NZ}}G_{\rm ret}^{(-)}(k_1,t). \tag{16}$$

In Eq. (16) $G_{\rm ret}^{(co)}(k,t)$ is

$$G_{\rm ret}^{(co)}(k,t)=u_k^2 G_{\rm ret}^{(+)}(k,t)+v_k^2 G_{\rm ret}^{(-)}(k,t), \tag{17}$$

where $G_{\rm ret}^{(+)}(k,t)$ and $G_{\rm ret}^{(-)}(k,t)$ are the Green's functions associated to the quasiparticles of the upper and the lower bands, respectively, with u_k^2 given by

$$u_k^2=\frac{1}{2}\left[1+\frac{\tilde{\epsilon}_k}{\sqrt{\tilde{\epsilon}_k^2+E^2}}\right] \tag{18}$$

and v_k^2 by

$$v_k^2=\frac{1}{2}\left[1-\frac{\tilde{\epsilon}_k}{\sqrt{\tilde{\epsilon}_k^2+E^2}}\right]. \tag{19}$$

One obtains the spectral function

$$A(k,\omega)=-2\,{\rm Im}\,G_{\rm ret}(k,\omega)=2\pi e^{-S}[u_k^2\delta(\omega-\xi_k^{(+)})+v_k^2\delta(\omega-\xi_k^{(+)})]+2\pi e^{-S}\sum_{n=0}^{\infty}\frac{S^n}{n!}[H(\omega-n\bar{\omega}_0)+H(-\omega-n\bar{\omega}_0)], \tag{20}$$

where the function $H(\omega)$ is

$$H(\omega)=\frac{g(\sqrt{\omega^2-E^2})}{\sqrt{1-\dfrac{E^2}{\omega^2}}}\,\theta(\omega-E)\,\theta(\sqrt{E^2+W^2}-\omega), \tag{21}$$

with $\theta(x)$ Heaviside function. Two physically distinct terms[26] appear in Eq. (20): the coherent and incoherent one. The first derives from the coherent motion of charge carriers and their surrounding phonon cloud. In the normal phase it represents the purely polaronic band contribution and shows a delta behavior. In the CO phase, this term is equal to the result of the mean-field approach when one neglects the renormalization of the upper and lower band due to the polaron effect. The incoherent term in Eq. (20) is due to processes changing the number of phonons during the hopping of the charges and provides a contribution spreading over a wide energy range.

In Fig. 2 we report the renormalized density of states $N(\omega)$ calculated in the ZFA approach (solid line) and mean-field (dashed line) at a fixed value of the el-ph coupling and $t=5\omega_0$. In the CO phase, a gap opens in the quasiparticle spectrum and it is larger for the mean-field solution than the ZFA one. We note that, at the energies corresponding to the gap, the inverse square-root singularity occurs for both approaches. The other sharp feature in the density of states derived in the ZFA approach is due to one-phonon processes

in the upper and lower bands that are relevant in the intermediate el-ph coupling regime.

III. OPTICAL PROPERTIES WITHIN ZFA APPROACH

In this section we focus our attention on the optical properties within the ZFA approach. Since we are primarily interested to the absorption spectra in the CO phase, we evaluate the conductivity for the frequency ω different from zero.

In a regime of linear response the real part of the conductivity is given by the current-current correlation function

$$\mathrm{Re}\,\sigma(\omega)=\lim_{\beta\to\infty}\left(\frac{1-e^{-\beta\omega}}{2\omega L}\right)\int_{-\infty}^{\infty}e^{i\omega t}\langle j^{\dagger}(t)j(0)\rangle, \quad (22)$$

where β is the inverse of the temperature and j the current operator. Performing the two canonical transformations (3),(5) and making the decoupling[26] of the correlation function in the electron and phonon terms through the introduction of H_{test} (9), we get

$$\langle j^{\dagger}(t)j(0)\rangle=\sum_{i,\delta}\sum_{i',\delta'}(\delta\cdot\delta')\Phi(i,i',\delta,\delta',t)\Delta(i,i',\delta,\delta',t), \quad (23)$$

where the function $\Delta(i,i',\delta,\delta',t)$ denotes the electron correlation function

$$\Delta(i,i',\delta,\delta',t)=\langle c_i^{\dagger}(t)c_{i+\delta}(t)c_{i'+\delta'}^{\dagger}c_{i'}\rangle_t \quad (24)$$

and the function $\Phi(i,i',\delta,\delta',t)$ the phonon correlation function

$$\Phi(i,i',\delta,\delta',t)=\langle X_i^{\dagger}(t)X_{i+\delta}(t)X_{i'+\delta'}^{\dagger}X_{i'}\rangle_t. \quad (25)$$

In order to simplify the analysis of our results, we separate Φ into two contributions

$$\begin{aligned}\Phi(i,i',\delta,\delta',t)&=[\langle X_i^{\dagger}X_{i+\delta\hat{\alpha}}\rangle_t]^2\{\Phi(i,i',\delta,\delta',t)\\&\quad-[\langle X_i^{\dagger}X_{i+\delta\hat{\alpha}}\rangle_t]^2\}\\&=e^{-2S}+[\Phi(i,i',\delta,\delta',t)-e^{-2S}], \quad (26)\end{aligned}$$

where S is given by Eq. (11).

Considering Eq. (26), the conductivity can be expressed as a sum of two terms[26]

$$\mathrm{Re}\,\sigma(\omega)=\mathrm{Re}\,\sigma^{(\mathrm{coh})}(\omega)+\mathrm{Re}\,\sigma^{(\mathrm{incoh})}(\omega). \quad (27)$$

As in the spectral properties, the appearance of two physically distinct contributions, the coherent and incoherent one, occurs. Actually the first term $\mathrm{Re}\,\sigma^{(\mathrm{coh})}$ is due to the charge transfer affected by the interactions with the lattice but not accompanied by processes changing the number of phonons. On the other hand, the incoherent term $\mathrm{Re}\,\sigma^{(\mathrm{incoh})}$ derives from inelastic scattering processes of emission and absorption of phonons. Both terms of the conductivity can be expressed in terms of the Green's function $G_{\mathrm{ret}}^{(co)}(k,t)$ given in Eq. (17).

The coherent conductivity is derived as

$$\mathrm{Re}\,\sigma^{(\mathrm{coh})}(\omega)=\left(\frac{4\pi e^2t^2}{\omega}\right)E^2e^{-2S}\int_{-\tilde{W}}^{0}d\epsilon\frac{g(\epsilon)}{(\xi^{(+)})^2}\left(1-\frac{\epsilon^2}{\tilde{W}^2}\right)\times\delta(\omega-2\xi^{(+)}), \quad (28)$$

with $\xi^{(+)}=\sqrt{\epsilon^2+E^2}$. We note that this term gives contribution to the conductivity only in the CO phase since it directly depends on the semigap E. Furthermore it is equal to the mean-field conductivity[12] when the renormalization of the upper and lower bands due to the polaron effect is neglected.

The incoherent term of the conductivity can be divided into two components:

$$\mathrm{Re}\,\sigma^{(\mathrm{incoh})}(\omega)=\mathrm{Re}\,\sigma_1^{(\mathrm{incoh})}(\omega)+\mathrm{Re}\,\sigma_2^{(\mathrm{incoh})}(\omega). \quad (29)$$

The quantity $\mathrm{Re}\,\sigma_1^{(\mathrm{incoh})}(\omega)$ is due to the multiphonon emission by the charge carriers in the lower band $\xi_k^{(-)}$ that does not change the electron momentum. This first term reads

$$\mathrm{Re}\,\sigma_1^{(\mathrm{incoh})}(\omega)=\frac{2\pi e^2t^2}{\omega}e^{-2S}\left[\frac{1}{L}\sum_{k\epsilon\mathrm{NZ}}\cos(k)(v_k^2-u_k^2)\right]^2\times\sum_{n=1}^{\infty}\frac{(2S)^n}{n!}\delta(\omega-n\bar{\omega}_0), \quad (30)$$

which, making the envelope of the delta functions (procedure exact in the limit $\omega_0\to 0$), becomes

$$\mathrm{Re}\,\sigma_1^{(\mathrm{incoh})}(\omega)=\frac{\pi e^2}{2\omega\bar{\omega}_0}\bar{E}_{\mathrm{kin}}^2\frac{(2S)^{\omega/\bar{\omega}_0}}{\Gamma(1+\omega/\bar{\omega}_0)}\theta(\omega-\bar{\omega}_0), \quad (31)$$

where $\bar{E}_{\mathrm{kin}}$ is the mean value of the kinetic energy equal to Eq. (14) and $\Gamma(x)$ is the gamma function.

In Eq. (29), $\mathrm{Re}\,\sigma_2^{(\mathrm{incoh})}(\omega)$ takes into account the interband transitions accompanied by multiphonon scattering. This second term is given by

$$\mathrm{Re}\,\sigma_2^{(\mathrm{incoh})}(\omega)=\frac{2\pi e^2t^2}{\omega}e^{-2S}\frac{1}{L}\sum_{k_1,k_2\epsilon\mathrm{NZ}}(1+4v_{k_1}u_{k_1}v_{k_2}u_{k_2})\times\sum_{n=1}^{\infty}\frac{(2S)^n}{n!}\delta(\omega-n\bar{\omega}_0+\xi_{k_1}^{(-)}-\xi_{k_2}^{(+)}), \quad (32)$$

which, enveloping the delta functions, can be transformed as

$$\mathrm{Re}\,\sigma_2^{(\mathrm{incoh})}(\omega)=\left(\frac{2\pi e^2t^2}{\omega\bar{\omega}_0}\right)e^{-2S}\int_{-\tilde{T}_1}^{0}d\epsilon_1\int_{-\tilde{T}_2}^{0}d\epsilon_2\frac{(2S)^y}{\Gamma(1+y)}\times g(\epsilon_1)g(\epsilon_2)\left(1+\frac{E^2}{4\xi_1^{(+)}\xi_2^{(+)}}\right)\times\theta(\omega-\bar{\omega}_0-2E), \quad (33)$$

where $T_1=\min[\tilde{W},\sqrt{(\omega-\bar{\omega}_0-E)^2-E^2}]$, $T_2=\min[\tilde{W},\sqrt{(\omega-\bar{\omega}_0-\xi_1^{(+)})^2-E^2}]$, $\xi_i^{(+)}$ is defined as

$$\xi_i^{(+)}=\sqrt{\epsilon_i^2+E^2}, \quad (34)$$

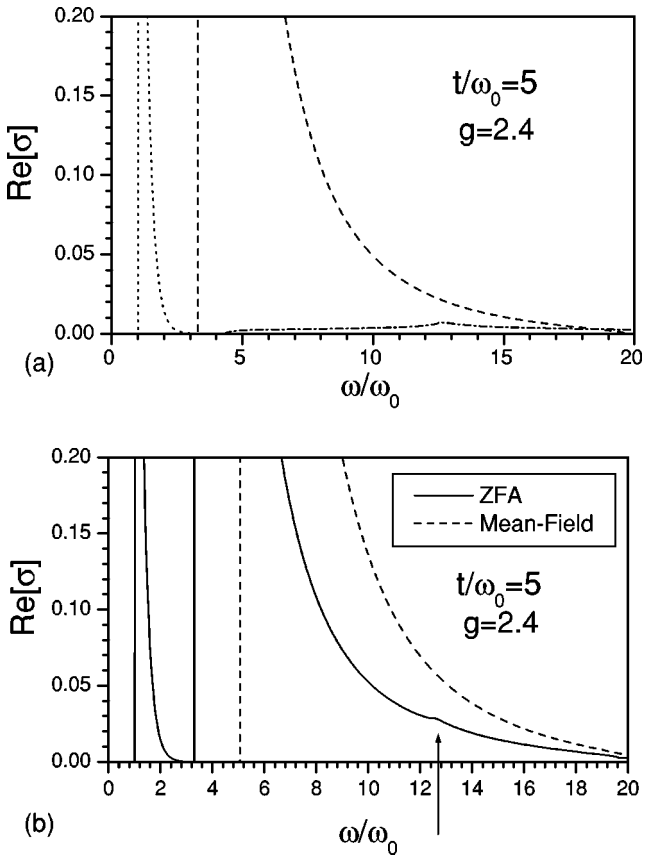

FIG. 3. (a) The conductivity at $t=5\omega_0$ and $g=2.4$ as a function of the frequency (in units of ω_0) decomposed into its different components: coherent term (dashed line), first incoherent term (dotted line) and second incoherent term (dash-dotted line). (b) The conductivity spectra derived in the ZFA (solid line) and mean-field approach (dashed line) at $t=5\omega_0$ and $g=2.4$ as a function of the frequency (in units of ω_0). The conductivities are expressed in units of $e^2\rho/mt$, with $m=1/2t$.

with $i=1,2,$ and $y=(\omega-\xi_1^{(+)}-\xi_2^{(+)})/\overline{\omega_0}$.

We have checked that the sum rule

$$\int_0^\infty d\omega \mathrm{Re}\,\sigma(\omega)=-\frac{\pi}{2}e^2\overline{E}_{\mathrm{kin}} \tag{35}$$

is verified by the calculated conductivity spectra in the CO phase, where $\overline{E}_{\mathrm{kin}}$ is given by Eq. (14).

In Fig. 3(a) we report the different contributions to the conductivity spectrum derived within the ZFA approach for $t=5\omega_0$ and $g=2.4$: the coherent term (dashed line), the incoherent term due to multiphonon emissions (dotted line) and the incoherent term in correspondence with interband transitions (dash-dotted line). For this value of the el-ph coupling, the gap is larger than the phonon frequency, that represents the absorption threshold of the first incoherent term. The incoherent term at ω_0 reaches the largest values in the intermediate coupling regime where one-phonon scattering processes are important. This contribution is still present for large el-ph couplings giving rise to a subgap absorption band. The second term of the incoherent conductivity spreads for a wide range of frequencies above the energy gap following the coherent interband absorption band.

In Fig. 3(b) the conductivity spectra within ZFA (solid line) and mean-field (dashed line) approaches at $t=5\omega_0$ and $g=2.4$ are compared. Not only the optical gap within ZFA is smaller than mean-field one, but the two incoherent terms due to lattice fluctuation effects are able to provide a non negligible contribution below and above the gap (the arrow in figure indicates this last contribution). This suggests that a better treatment of the lattice fluctuations allows to capture features of the optical conductivities that are found in experimental spectra.[13] In the next section we will see that lattice fluctuation effects beyond the ZFA approach give rise in the conductivity to an actual subgap tail in good agreement with experimental data.

With rising the el-ph coupling, a transfer of spectral weight from low to high energies takes place and the optical gap broadens. The optical response within ZFA approach is strongly dependent on adiabaticity ratio since the incoherent terms acquire increasing spectral weight compared with that of the coherent interband term as the ratio t/ω_0 decreases. This transfer of spectral weight can be measured through the ω-integrated function

$$S(\omega)=\int_0^\omega d\omega' \mathrm{Re}\,\sigma(\omega'), \tag{36}$$

whose value S_m in the limit of infinite frequency is given by Eq. (35).

IV. FLUCTUATIONS BEYOND ZFA APPROACH

In this section we deal with quantum lattice fluctuation effects beyond the ZFA approach. We first determine the scattering rate of the quasiparticles of the upper and lower bands. Next we will analyze the effect of the self-energy insertions on the infrared conductivity that is the main aim of this paper. This is performed following the lines of our previous works.[26,27]

Now we consider the actual transformed Hamiltonian of the system in Eq. (6) as a perturbation of the test Hamiltonian in Eq. (9). At the second order of the perturbation theory the retarded self-energy $\Sigma_{\mathrm{ret}}^{(2)}(k,\omega)$ can be derived.[28–32] If only the dominant autocorrelation terms are retained, the self-energy is local and provides the scattering rates of the quasiparticles of the upper and lower bands

$$\Gamma_{\pm}(k)=-2\,\mathrm{Im}\,\Sigma_{\mathrm{ret}}^{(2)}(\omega=\xi_k^{(\pm)}). \tag{37}$$

These two quantities turn out to be equal, so we have only one scattering rate

$$\Gamma(k)=\Gamma_+(k)=\Gamma_-(k). \tag{38}$$

The scattering rate can be decomposed as

$$\Gamma(k)=\Gamma(\xi_k^{(+)})=\Gamma_{1\text{-phon}}(\xi_k^{(+)})+\Gamma_{\mathrm{multiphon}}(\xi_k^{(+)}), \tag{39}$$

where $\Gamma_{1\text{-phon}}$ is the contribution due to single phonon processes only

$$\Gamma_{1\text{-phon}}(\xi_k^{(+)}) = 2Zt^2 e^{-2S} g^2 f^2 e^{-4\alpha} g_{1,l=1}(\xi_k^{(+)}) + g^2\omega_0^2 e^{4\alpha}(1-f)^2 g_2(\xi_k^{(+)}), \quad (40)$$

$\Gamma_{\text{multiphon}}$ represents the scattering rate by multiphonon processes

$$\Gamma_{\text{multiphon}}(\xi_k^{(+)}) = Zt^2 e^{-2S} \sum_{l=2}^{+\infty} \frac{(2g^2 f^2 e^{-4\alpha})^l}{l!} g_{1,l}(\xi_k^{(+)}). \quad (41)$$

In the previous equations the function $g_{1,l}(\xi_k^{(+)})$ reads

$$g_{1,l}(\xi_k^{(+)}) = [n_F(\xi_k^{(+)} + l\overline{\omega_0})]K(\xi_k^{(+)} + l\overline{\omega_0}) + [1 - n_F(\xi_k^{(+)} - l\overline{\omega_0})]K(\xi_k^{(+)} - l\overline{\omega_0}) \quad (42)$$

and $g_2(\xi_{\mathbf{k}}^{(+)})$

$$g_2(\xi_{\mathbf{k}}^{(+)}) = [n_F(\xi_k^{(+)} + \overline{\omega_0})]B(\xi_{\mathbf{k}}^{(+)} + \overline{\omega_0}) + [1 - n_F(\xi_k^{(+)} - \overline{\omega_0})]B(\xi_k^{(+)} - \overline{\omega_0}), \quad (43)$$

where $B(x) = 2\pi[H(x) + H(-x)]$, with $H(x)$ given in Eq. (21). In the CO phase the scattering rate has a gap due to the dimerization and the process of phonon spontaneous emission by the quasiparticles.[27]

The role of the scattering rate is important not only to improve the approximations of calculation of the spectral properties, but also the optical properties. Through the scattering rate, we can consider the new Green's function $\tilde{G}_{\text{ret}}^{(co)}(k,t)$

$$\tilde{G}_{\text{ret}}^{(co)}(k,t) = u_k^2 \tilde{G}_{\text{ret}}^{(+)}(k,t) + v_k^2 \tilde{G}_{\text{ret}}^{(-)}(k,t), \quad (44)$$

that substitutes the function $G_{\text{ret}}^{(co)}(k,t)$ given in Eq. (17). In Eq. (44) the Green' functions $\tilde{G}_{\text{ret}}^{(\nu)}(k,t)$ are

$$\tilde{G}_{\text{ret}}^{(\nu)}(k,t) = -i\theta(t)\exp(-i\xi_k^{(\nu)}t)\exp[-t\Gamma(k)/2], \quad (45)$$

with ν standing for $+$ or $-$. Therefore it is possible to derive a new spectral function and density of states that include lattice fluctuation effects beyond the ZFA approach. A pseudogap as precursor of the actual gap at stronger el-ph couplings is found in the density of states.[27]

The inclusion of the scattering rate is able to affect the features of the infrared absorption. As in the ZFA approach, the conductivity is decomposed into a coherent and an incoherent term:

$$\text{Re}\,\sigma_{\text{fluct}}(\omega) = \text{Re}\,\sigma_{\text{fluct}}^{(\text{coh})}(\omega) + \text{Re}\,\sigma_{\text{fluct}}^{(\text{incoh})}(\omega). \quad (46)$$

The coherent conductivity is given by

$$\text{Re}\,\sigma_{\text{fluct}}^{(\text{coh})}(\omega) = \left(\frac{4e^2t^2}{\omega}\right) e^{-2S} \sum_{\nu_1,\nu_2} \int_{-\tilde{W}}^{0} d\epsilon [n_F(\xi^{(\nu_1)} - \omega) - n_F(\xi^{(\nu_1)})] \tilde{C}^{(\nu_1,\nu_2)}(\epsilon,\omega) h(\epsilon) A^{(\nu_1,\nu_2)}(\epsilon), \quad (47)$$

where $\tilde{C}^{(\nu_1,\nu_2)}(\epsilon,\omega)$ is

$$\tilde{C}^{(\nu_1,\nu_2)}(\epsilon,\omega) = \frac{\Gamma(\epsilon)}{\Gamma^2(\epsilon) + (\xi^{(\nu_2)} - \xi^{(\nu_1)} + \omega)^2}, \quad (48)$$

$h(\epsilon) = g(\epsilon)(1 - \epsilon^2/4t_{\text{eff}}^2)$, with $g(\epsilon)$ bare density of states, and the function $A^{(\nu_1,\nu_2)}(\epsilon)$ is expressed by

$$A^{(+,+)}(\epsilon) = A^{(-,-)}(\epsilon) = \frac{\epsilon^2}{\epsilon^2 + E^2} \quad (49)$$

and

$$A^{(+,-)}(\epsilon) = A^{(-,+)}(\epsilon) = \frac{E^2}{\epsilon^2 + E^2}. \quad (50)$$

The latter term of the conductivity becomes

$$\text{Re}\,\sigma_{\text{fluct}}^{(\text{incoh})}(\omega) = \left(\frac{2e^2t^2}{\omega}\right) e^{-2S_T} \sum_{\nu_1,\nu_2} \int_{-\tilde{W}}^{0} d\epsilon \int_{-\tilde{W}}^{0} d\epsilon_1 g(\epsilon) \times g(\epsilon_1) R^{(\nu_1,\nu_2)}(\epsilon,\epsilon_1,\omega), \quad (51)$$

where the function $R^{(\nu_1,\nu_2)}(\epsilon,\epsilon_1,\omega)$ is given by

$$R^{(\nu_1,\nu_2)}(\epsilon,\epsilon_1,\omega) = \sum_{l=1}^{+\infty} \frac{(2g^2 f^2 e^{-4\alpha})^l}{l!} [J_l^{(\nu_1,\nu_2)}(\epsilon,\epsilon_1,\omega) + H_l^{(\nu_1,\nu_2)}(\epsilon,\epsilon_1,\omega)], \quad (52)$$

$C^{(\nu_1,\nu_2)}(\epsilon,\epsilon_1,x)$ is

$$C^{(\nu_1,\nu_2)}(\epsilon,\epsilon_1,x) = \frac{1}{2} \frac{[\Gamma(\epsilon) + \Gamma(\epsilon_1)]}{[\Gamma(\epsilon) + \Gamma(\epsilon_1)]^2/4 + (\xi^{(\nu_1)} - \xi_1^{(\nu_2)} + x)^2}, \quad (53)$$

and

$$\xi_i^{(\nu_j)} = \nu_j \sqrt{\epsilon_i^2 + E^2}. \quad (54)$$

In Eq. (51) the functions $J_l^{(\nu_1,\nu_2)}(\epsilon,\epsilon_1,\omega)$

$$J_l^{(\nu_1,\nu_2)}(\epsilon,\epsilon_1,\omega) = C^{(\nu_1,\nu_2)}(\epsilon,\epsilon_1,\omega + l\overline{\omega_0})[n_F(\xi_1^{(\nu_2)} - l\overline{\omega_0} - \omega) - n_F(\xi_1^{(\nu_2)} - l\overline{\omega_0})]n_F(\xi_1^{(\nu_2)}) \quad (55)$$

and $H_l^{(\nu_1,\nu_2)}(\epsilon,\epsilon_1,\omega)$

$$H_l^{(\nu_1,\nu_2)}(\epsilon,\epsilon_1,\omega) = C^{(\nu_1,\nu_2)}(\epsilon,\epsilon_1,\omega - l\overline{\omega_0})[n_F(\xi_1^{(\nu_2)} + l\overline{\omega_0} - \omega) - n_F(\xi_1^{(\nu_2)} + l\overline{\omega_0})][1 - n_F(\xi_1^{(\nu_2)})] \quad (56)$$

describe phonon scattering processes.

In Fig. 4 we show the conductivity at $t = 10\omega_0$ and $\lambda = 0.45$: the solid line represents the quantity obtained adding fluctuations over ZFA, the dashed line that derived within ZFA, and dotted line that of the mean-field approach. The values of the parameters have been chosen such that they are appropriate for quasi-1D inorganic metals. First we observe

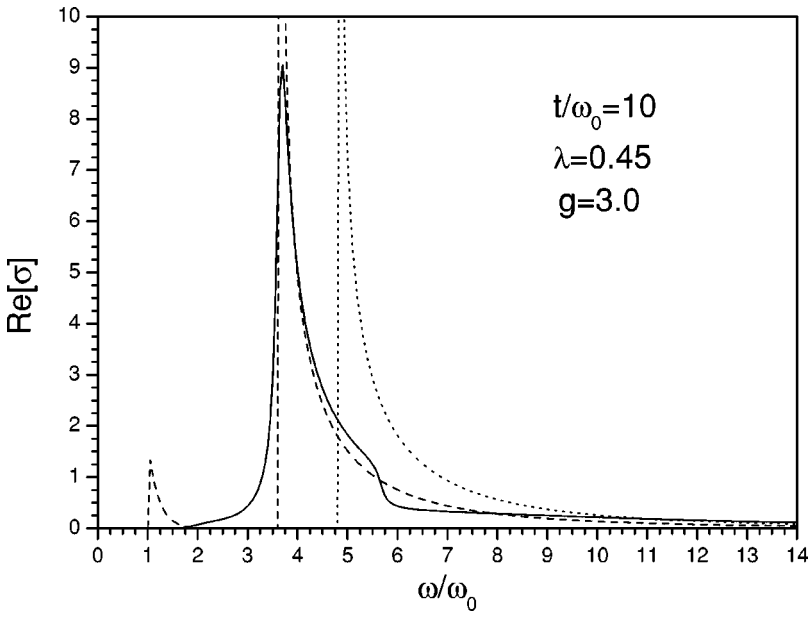

FIG. 4. The conductivity (in units of $e^2\rho/mt$, with $m=1/2t$) obtained including fluctuations beyond the ZFA (solid line), derived in the ZFA (dashed line), and in the mean-field approach (dotted line) up to 14 ω_0 at $t=10\omega_0$ and $\lambda=0.45$.

that the inverse square-root singularity obtained in the mean-field and ZFA approach is reduced. Then, due to quantum lattice fluctuations, the new conductivity not only shows a long subgap tail but presents anomalies also over the gap when compared with the mean-field spectrum. Therefore it strengthens the tendencies already shown by the ZFA conductivity and it is in good agreement with the experimental spectra.[6,13,14]

As stressed in the introduction, an analytical variational approach,[21,22] valid in the weak el-ph coupling regime and based on a similar procedure of calculation, has been developed to study the optical conductivity. In order to emphasize the different physical results between the present work and the previous one, in Fig. 5 we compare the conductivity $\mathrm{Re}\,\sigma_{\mathrm{fluct}}$ (solid line) with the corresponding quantity (dashed line) obtained within the preceding approach[22] for $t=10\omega_0$ and $\lambda=1$. This last conductivity is extrapolated from the weak coupling limit and, as already noted by the authors of the work, it shows a maximum that does not coincide with their energy gap (see dashed arrow in the figure). This feature is not consistent with experimental spectra[13] that, at $T=0$, show the maximum of the infrared optical conductivity generally near to the gap determined by other experimental measurements such as the low-temperature resistivity, the temperature dependence of the susceptibility and neutron and Raman scattering.[14] As clearly shown in Fig. 5, our approach is not affected by this problem. While in the previous work[22] the presence of a tail below the peak should be due to usual interband transitions, in our approach the peak in the conductivity corresponds to the gap in the quasiparticle spectrum and is well above a real subgap tail determined by lattice fluctuations.

In the inset of Fig. 5 we report the ratio (solid line) between $S(\omega)$, the spectral weight of the conductivity calculated in this section, and S_m, the same quantity in the limit of infinite frequency. This ratio is compared with that (dashed line) obtained by means of exact diagonalizations of the Hamiltonian for a system of six sites.[24] Our approach cap-

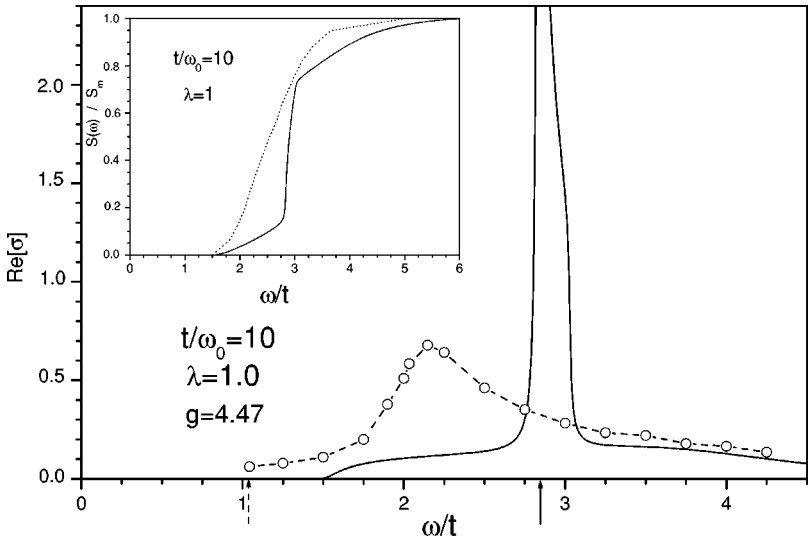

FIG. 5. The conductivity of the present approach (solid line) in comparison with that (dashed line) calculated in a previous paper (Ref. 22) at $t=10\omega_0$ and $\lambda=1.0$. The solid arrow indicates the gap in our approach and the dashed arrow that obtained in a previous work (Ref. 22). In the inset the ratio between the spectral weight $S(\omega)$ and S_m calculated in the present approach (solid line) compared with the same quantity (dashed line) derived from exact numerical diagonalizations.[24]

tures the correct onset of the optical response, even if it presents sharper features. This could be due to the fact that we are not considering a small cluster but we are performing the thermodynamic limit, and, furthermore, that higher order self-energy insertions should be included in order to improve the approach.

The optical response shows similar features at lower values of the adiabaticity ratio t/ω_0. In the regime of near electronic and phononic energy scales the effects due to lattice fluctuations are enhanced and the contributions below and above the gap subtract a larger spectral weight to the interband gap term. This regime is typically important for inorganic linear chain compounds, for example, the compound TTF-TCNQ, that is a narrow-band one-dimensional metal with a relatively strong el-ph coupling.[33]

V. CONCLUSIONS

We have discussed the optical properties of the half-filled spinless Holstein model in the 1D case at zero temperature within the ZFA approach. We have observed that, with increasing the el-ph coupling, the ordered phase affects the conductivity spectra inducing a transfer of spectral weight from low to high energies and a broadening of the optical interband gap. The quantum lattice fluctuations considered in the ZFA approach are able to affect the optical response of the system that shows bands below and above the gap. When fluctuation effects beyond the ZFA approach are included, the optical conductivities are profoundly changed since they are characterized by a subgap tail and a wide band above the interband optical gap term that is smoothed when compared with the mean-field result. Therefore the inelastic scattering processes influence the low-frequency and high-frequency features of the conductivity in agreement with experimental spectra.[13,14] Our results make clear that a treatment of the lattice fluctuations beyond the ZFA approach is required to obtain a consistent agreement with experimental data.

In this paper lattice fluctuation effects beyond the ZFA approach are included calculating perturbatively the scattering rate of the polarons that form the ordered state. A second-order perturbation calculation on the ZFA solution reproduces the integrated spectral weights obtained by exact numerical approaches suggesting that the employed approach can capture the infrared response of the model. Finally we note that our approach is valid in the infrared range of frequencies where the interband absorption typically takes place. Thus it is not able to reveal the structures attributed to collective excitation modes arising from the CDW condensate.[1,9,10]

[1] G. Grüner, in *Density Waves in Solids* (Addison-Wesley, Reading, MA, 1994).

[2] *Charge Density Waves in Solids*, edited by Gy. Hutiray and J. Sólyom (Springer-Verlag, Heidelberg, 1985).

[3] *One-Dimensional Conductors*, by S. Kagoshima, H. Nagasawa, and T. Sambongi (Springer-Verlag, New York, 1988).

[4] G. Traviglini *et al.*, Solid State Commun. **37**, 599 (1981).

[5] N. Tsuda, K. Nasu, A. Yanese, and K. Siratori, *Electronic Conduction in Oxides* (Springer-Verlag, Berlin, 1990); *Organic Conductors*, edited by J.-P. Farges (Dekker, New York, 1994).

[6] R.H. McKenzie and J.W. Wilkins, Phys. Rev. Lett. **69**, 1085 (1992).

[7] K. Kim, R.H. McKenzie, and J.W. Wilkins, Phys. Rev. Lett. **71**, 4015 (1993).

[8] L. Perfetti, H. Berger, A. Reginelli, L. Degiorgi, H. Höchst, J. Voit, G. Margaritondo, and M. Grioni, Phys. Rev. Lett. **87**, 216404 (2001).

[9] G. Grüner, Rev. Mod. Phys. **60**, 1129 (1988).

[10] L. Degiorgi, B. Alavi, G. Mihály, and G. Grüner, Phys. Rev. B **44**, 7808 (1991).

[11] V. Vescoli, L. Degiorgi, H. Berger, and L. Forró, Phys. Rev. Lett. **81**, 453 (1998).

[12] P.A. Lee, T.M. Rice, and P.W. Anderson, Solid State Commun. **14**, 703 (1974).

[13] L. Degiorgi, St. Thieme, B. Alavi, G. Grüner, R. H. McKenzie, K. Kim, and F. Levy, Phys. Rev. B **52**, 5603 (1995).

[14] A. Schwartz, M. Dressel, B. Alavi, A. Blank, S. Dubois, G. Grüner, B.P. Gorshunov, A.A. Volkov, G.V. Kozlov, S. Thieme, L. Degiorgi, and F. Lévy, Phys. Rev. B **52**, 5643 (1995).

[15] T. Holstein, Ann. Phys. (Leipzig) **8**, 325 (1959); **8**, 343 (1959).

[16] J.E. Hirsch and E. Fradkin, Phys. Rev. Lett. **49**, 402 (1982); J.E. Hirsch and E. Fradkin, Phys. Rev. B **27**, 4302 (1983).

[17] R.H. McKenzie, C.J. Hamer, and D.W. Murray, Phys. Rev. B **53**, 9676 (1996).

[18] C. Bourbonnais and L.G. Caron, J. Phys. (Paris) **50**, 2751 (1989).

[19] D. Schmeltzer, J. Phys. C **18**, L1103 (1985).

[20] H. Zheng, D. Feinberg, and M. Avignon, Phys. Rev. B **39**, 9405 (1989).

[21] H. Zheng and M. Avignon, Phys. Rev. B **58**, 3704 (1998).

[22] Q. Wang, H. Zheng, and M. Avignon, Phys. Rev. B **63**, 14 305 (2000).

[23] R.J. Bursill, R.H. McKenzie, and C.J. Hamer, Phys. Rev. Lett. **80**, 5607 (1998).

[24] A. Weisse and H. Fehske, Phys. Rev. B **58**, 13 526 (1998).

[25] I. J. Lang and Yu. A. Firsov, Sov. Phys. JETP **16**, 1301 (1963); Yu. A. Firsov, *Polarons* (Nauka, Moscow, 1975).

[26] C.A. Perroni, G. De Filippis, V. Cataudella, and G. Iadonisi, Phys. Rev. B **64**, 144302 (2001).

[27] C.A. Perroni, V. Cataudella, G. De Filippis, G. Iadonisi, V. Marigliano Ramaglia, and F. Ventriglia, Phys. Rev. B **67**, 094302 (2003).

[28] J. Schnakenberg, Z. Phys. **190**, 209 (1966).

[29] J. Loos, Z. Phys. B: Condens. Matter **92**, 377 (1993).

[30] J. Loos, Z. Phys. B: Condens. Matter **96**, 149 (1994).

[31] L. P. Kadanoff and G. Baym, *Quantum Statistical Mechanics* (Benjamin/Cumming, Reading, MA, 1962).

[32] H. Fehske, J. Loss, and G. Wellein, Z. Phys. B: Condens. Matter **104**, 619 (1997).

[33] A. J. Heeger, in *Highly Conducting One-Dimensional Solids*, edited by J.T. Devreese, R.P. Evrard, and V.E. van Doren (Plenum Press, New York, 1979).